



**Environmental  
Science**  
Nano

**Uptake of Polystyrene Nanospheres by Wheat and Arabidopsis Roots in Agar, Hydroponics, and Soil**

Journal:	<i>Environmental Science: Nano</i>
Manuscript ID	EN-ART-12-2024-001182
Article Type:	Paper

SCHOLARONE™  
Manuscripts

# Environmental Science Nano

## PAPER

Cite this: DOI: 00.0000/xxxxxxxxxx

## Uptake of Polystyrene Nanospheres by Wheat and Arabidopsis Roots in Agar, Hydroponics, and Soil<sup>†</sup>

Kaushik Adhikari<sup>a,b</sup>, Karen A. Sanguinet<sup>b</sup>, Carolyn I. Pearce<sup>c</sup>, Markus Flury<sup>a,b\*</sup>

Received Date

Accepted Date

DOI: 00.0000/xxxxxxxxxx

Plant uptake of micro- and nanoplastics can lead to contamination of food with plastic particles and subsequent human consumption of plastics. There is evidence that plant roots can take up micro- and nanoplastics; however, most of this evidence stems from experiments conducted with plants grown in hydroponics or agar systems where uptake of nanoparticles by roots is more favorable than when plants were grown in soil. Here, we discern the root uptake and accumulation of polystyrene nanospheres in plants grown in different growing media: agar, hydroponics, and soil. In addition, we tested the impacts of nanospheres on plant biomass and plant stress. Wheat and *Arabidopsis thaliana* were grown in agar, hydroponics, and soil media and exposed to polystyrene nanospheres. Three different nanospheres were used (40 nm and 200 nm carboxylate-modified and 200 nm amino-modified polystyrene) and uniformly mixed into the growing media. Plants were grown for 7 to 10 days and roots were then examined for the presence of nanospheres by confocal laser scanning microscopy and scanning electron microscopy. Plant stress was evaluated by measuring reactive oxygen species (ROS). We observed the 40 nm nanospheres inside plant roots, but the 200 nm nanospheres only adhered to root cap cells showing no uptake into the roots. Furthermore, confocal images indicated that root uptake of nanospheres was favored in hydroponic solutions as compared to agar and soil media. Plant biomass was generally not affected by the nanospheres, except for hydroponically grown *A. thaliana*, where biomass was significantly reduced. Small sized (40 nm) and positively charged (200 nm amino-modified) nanospheres showed higher ROS accumulation in plants than negatively charged 200 nm carboxylate-modified nanospheres. This study provides evidence that polystyrene nanospheres can be taken up into the interior of plant roots and cause plant stress, but these impacts are less pronounced in media where the plastic particles are less mobile, like in agar and soil media as compared to hydroponic systems.

### Environmental significance

Micro- and nanoplastics pose a threat to terrestrial ecosystems because they can impair soil and plant health. Micro- and nanoplastics have been shown to be taken up by plants through roots, and this provides a pathway for human exposure when plants are consumed. Most of the evidence of root uptake of micro- and nanoplastics stems from hydroponic systems; however, when plants are grown in soil media, then uptake of plastic particles by roots is likely less pronounced than in hydroponics because plastic particles attach to soil particles and are less plant available. Our findings provide experimental evidence that this is indeed the case, as less plastic particles were taken up by roots grown in soil as compared to hydroponics. Plants grown in hydroponics thus are more susceptible to plastic particle uptake than plants grown in soil.

<sup>a</sup> Department of Crop & Soil Sciences, Puyallup Research & Extension Center, Washington State University, Puyallup, WA 98371, USA.

<sup>b</sup> Department of Crop & Soil Sciences, Washington State University, Pullman, WA 99164, USA.

<sup>c</sup> Pacific Northwest National Laboratory, Richland, WA 99354, USA.

<sup>†</sup> Electronic Supplementary Information (ESI) available: Details on confocal microscopy settings, biomass measurements, statistics, images of polystyrene nanospheres, experimental setups, and confocal z-stack images. See DOI:

## 1 Introduction

Agricultural soils receive nano- and microplastics from different sources such as biosolids application, compost amendments, plastic mulching, irrigation water, and atmospheric deposition<sup>1–3</sup>. Nano- and microplastics can be translocated into the root zone by infiltrating water, tillage, or bioturbation<sup>4</sup>. Crops are therefore inevitably exposed to nano- and microplastics present in soils. If nano- and microplastics are taken up by roots and transferred to the edible parts of the plants, then the plastic particles are being introduced into the food chain and subject to human consumption.

Nano- and microplastics can enter plant roots by two main pathways: the apoplastic and symplastic pathway. The apoplastic pathway is the entry of nano- and microplastics through the spaces between root cells, driven by water movement, but the interior of the cells is not penetrated. This pathway is mainly affected by transpiration rate<sup>5,6</sup>. The symplastic pathway involves the transport of plastic particles through plasmodesmata and the entry of the particles into the cytoplasm of the root cells. This transport mechanism is usually considered to have a size exclusion limit of 40 to 50 nm<sup>7</sup>. A third, less common mode of plant uptake is the entry of plastic particles through cracks formed in the root tissue during lateral root emergence, i.e., crack entry mode uptake<sup>5</sup>. After plastics accumulate in the vascular tissue inside plant roots, they can also be translocated to the stem and leaves<sup>8</sup>.

Plant uptake of nano- and microplastics has mainly been studied with model spherical polystyrene particles, ranging from 40 to 2000 nm, and having negative or positive surface charge. The experimental conditions mostly involved growing plants in nutrient solutions spiked with polystyrene nano- and microplastics, either in agar or hydroponic systems. Sun et al.<sup>6</sup> observed limited root uptake of positively charged 265 nm polystyrene spheres, but more uptake of negatively charged 200 nm spheres into the epidermal root tissue and the xylem of *Arabidopsis thaliana*. Li et al.<sup>5</sup>, also working with hydroponic systems, observed apoplastic transport of negatively charged 200 and 2000 nm polystyrene spheres, but no penetration beyond the Casparian strip in *Triticum aestivum* and *Lactuca sativa*. However, where the Casparian strip was not intact, i.e., where lateral roots emerge from the main root, polystyrene spheres could enter the vascular tissue of the roots and be translocated to the shoot. This uptake via crack entry mode was postulated as a main mechanism for uptake of plastic by roots, allowing particles up to 2000 nm to enter the vascular system<sup>5</sup>.

An important factor that affects the root uptake of nano- and microplastic is the surface charge, which determines how the plastic particles interact with plant cells. Plant roots produce mucilage and exudates, which are negatively charged, and which stick to positively charged nano- and microplastics and inhibit penetration into the root<sup>9</sup>. Indeed, the translocation of negatively charged polystyrene nanospheres to different plant parts

was more prominent than that of positively charged nanospheres in *A. thaliana* grown in half-strength MS medium<sup>6</sup>. Nonetheless, positively charged polystyrene nanospheres induced oxidative stress, inhibited seedling development, and plant growth<sup>6</sup>.

Hydroponic systems have been used in most studies where uptake of polystyrene spheres into roots has been reported<sup>5,6,10–13</sup>. Using TEM imaging, Dong et al.<sup>10</sup> detected 200 and 1000 nm polystyrene nanoparticles in the root cortex of *Daucus carota* L., but only the 200 nm spheres were observed in the stele and xylem. Also using TEM imaging, Spano et al.<sup>11</sup> found that 50 nm polystyrene nanoparticles could penetrate into the cytoplasm and vacuoles of *Oryza sativa* L. Fifty nanometer polystyrene nanoparticles were found to accumulate inside plant roots when grown in vermiculite and half strength Murashige and Skoog (MS) solution<sup>14</sup>.

Hydroponic systems are most conducive for root uptake of nano- and microplastics because plastic particles are highly mobile and have frequent contact with plant roots. However, when plants are grown in agar or soil, nano- and microplastics are not as mobile and are not readily available for root uptake. Indeed, no uptake of polystyrene spheres (40 and 1000 nm) was observed when *A. thaliana* and *Triticum aestivum* were grown in agar media; but rather, the polystyrene spheres accumulated at the root cap cells when the roots pushed their way through the agar medium<sup>15</sup>. In real soils, plastic particles are usually attached to soil particles and thus are even less readily available for root uptake.

The overall goal of this study is to assess the interaction and accumulation of polystyrene nano- and microplastics in *A. thaliana* and wheat plants under different growth conditions (agar, hydroponics, and soil). We hypothesized that root uptake of nano- and microplastics depends on the system in which the plants are grown, following the sequence: hydroponics > agar > soil, with limited root uptake in soils. We further tested the effect of plastic size (40 and 200 nm) and surface charge (positive and negative) on the potential root uptake and accumulation on and inside the roots, and whether the plastic particles induce oxidative stress.

## 2 Materials and Methods

### 2.1 Plastic materials and characterization

Two different sizes (40 and 200 nm) of yellow-green fluorescent polystyrene nanospheres with two different surface modifications, negatively charged carboxylate- and positively charged amino-modified spheres, were used (Table 1, Figure S1). Excitation and emission wavelengths for the spheres are 505 and 515 nm, respectively. Polystyrene nanospheres, as purchased, were stored in a refrigerator at 4°C. The 200 nm carboxylate- and amino- modified polystyrene microspheres contained sodium azide as a preservative, and to remove the sodium azide, we dialyzed a suspension of 0.29 g/L with a 25 mm 12,000–14,000 MWCO dialysis membrane (Spectra/Por, Spectrum Laboratories, Inc., Rancho Domingues, CA) in deionized water for 3 days. The zeta-potentials of the nanospheres were measured with a Zetasizer (Zetasizer Nano ZS (Malvern Instruments Ltd., Malvern, UK) in deionized water and half-strength Murashige and Skoog (MS)

00.0000/00000000.

Table 1 Characteristics of polystyrene nanospheres. Spheres were obtained from ThermoFisher Scientific, USA.

Particle Diameter (nm)	Surface Modification	Color	Excitation (nm)	Emission (peak) (nm)	Zeta Potential <sup>†</sup> (mV)	Stock Concentration (g/mL)	Lot Nr.
40	carboxylate (-OOH)	yellow-green	505	515	-60.0 ± 2.9	0.05	F8795
200	carboxylate (-OOH)	yellow-green	505	515	-21.4 ± 1.8	0.02	F8811
200	amino (-NH <sub>2</sub> )	yellow-green	505	515	7.8 ± 4.1	0.02	F8764

<sup>†</sup> Zeta potential of the spheres measured in distilled water with a Zetasizer Nano ZS (Malvern Instruments Ltd., Malvern, UK). Data are mean and standard deviations of 10 measurements.

solution<sup>16</sup>, consisting of macro- and micronutrients and vitamins.

## 2.2 Plant growth experiments

**Plants:** Two model plants were used, (i) soft white spring wheat cv. Louise (*Triticum aestivum*), representing a monocot with a fibrous root system, and (ii) *Arabidopsis* (*A. thaliana* ecotype Columbia), representing a dicot with a tap root. The seeds of wheat and *A. thaliana* were washed with 20% bleach and Triton X-100 (Sigma-Aldrich) solution for 10 minutes, followed by rinsing three times with ultra-pure water, then a 70% ethanol solution was added to the seeds for 2 minutes, and finally the seeds were rinsed thoroughly with ultra-pure water<sup>15</sup>. The seeds were then stored in ultra-pure water at 4°C for three days for cold stratification.

**Growth media:** Plants were exposed to the nanospheres in three different growth media: agar, hydroponics, and soil. These three media were chosen to represent different uptake scenarios: In agar, nanospheres are immobile, embedded in the semi-solid agar medium, and as such the nanospheres cannot move towards roots, so that root-nanosphere contact can only occur via root interception. In hydroponics, nanospheres are freely mobile and frequent root-nanosphere contact occurs via diffusion and convection (through transpiration). In soil, root-nanosphere contact occurs via a combination of interception and diffusion-convection, superimposed by the interactions of the nanospheres with the soil matrix.

For agar, plants were grown in sterile Petri dishes, for hydroponics, plants were grown in Magenta boxes (PhytoTech Labs, Inc., Lenexa, KS, USA), and for the soil experiments, plants were grown in clay pots and in micro-ROCs (microscopy Rhizosphere Observation Chambers)<sup>17</sup> filled with soil medium (Figures S2, S3). All growth experiments were conducted in a growth chamber. The exposure concentrations for the nanoplastics in all the growth media were chosen as 0.029 g/L or  $8.3 \times 10^{11}$  n/mL for the 40 nm spheres and 0.029 g/L or  $6.6 \times 10^9$  n/mL for the 200 nm spheres, where the volume refers to the volume of liquid, agar, or soil medium. These concentrations were chosen based on our previous experiments<sup>15</sup> and ensure good visualization of the nanospheres with confocal microscopy.

**Agar:** For the experiments with agar, the seeds were placed into sterile Petri dishes (Fisherbrand, 08-757-11A or -12, Fisher Scientific) containing 25 mL autoclaved growth medium (half-strength MS solution with 0.7% agar) and fluorescent nanospheres. First, nanospheres were mixed with half-strength MS media (PhytoTech Labs, Lenexa, KS) at the specified concentration (0.029 g/L), and

then sonicated for 10 minutes. Agar (Bacto Agar, Becton, Dickinson and Company, Sparks, MD) was added to the mixture. Five and ten seeds of wheat and *A. thaliana* plants, respectively, were used for each experiment. Control samples, containing only seeds with growth medium but no nanospheres, were also prepared. Petri dishes with seeds placed on top of the agar were sealed, and transferred to a growth chamber with growing conditions of a day/night cycle of 16/8 h with temperatures of 22°C/18°C day/night. Wheat was grown in a growth chamber for 10 days, *A. thaliana* was grown for 7 days. These time periods were chosen based on our previous experience<sup>15</sup>, namely that roots were grown sufficiently but not too large for good visualization with confocal microscopy. The plants were then pulled out from the growth medium with a tweezer and placed on a microscopy slide with a few drops of half-strength MS solution, covered with a cover slide, and analyzed with confocal laser scanning microscopy and scanning electron microscopy (SEM). One set of plant roots was washed by dipping the roots into clean half-strength MS solution and moving the roots up and down 6 times. Each treatment was replicated three times, and for each replicate three wheat plants and six *A. thaliana* plants were imaged with confocal microscopy, and three wheat plants were used for root cross-sectioning and SEM imaging.

**Hydroponics:** For hydroponics, wheat seeds were germinated on autoclaved growth medium (half-strength MS solution with 0.7% agar) in Petri dishes for 2 days, and then the seedlings were transferred to the hydroponic system in a laminar flow hood. For *A. thaliana*, seeds were directly germinated in the hydroponic system. The hydroponic system consisted of a 385 mL Magenta GA-7 tissue culture vessel (Sigma-Aldrich) filled with 200 mL half MS solution for wheat and 100 mL for *A. thaliana*, with and without nanospheres. On top of the hydroponic solutions, we placed a stainless steel mesh (304 Stainless Steel Mesh Screen, ELAFROS, Amazon) which supported the seedlings. The culture vessels were then covered with caps, and placed inside a growth chamber under the same growth conditions as used for the agar media experiments. After 10 days for wheat and 7 days for *A. thaliana*, the plants were removed with a tweezer and then analyzed with confocal laser scanning microscopy and SEM imaging in the same manner as the plants in the agar experiments.

**Soil:** For the soil medium, an oven dried greenhouse soil mix (professional growing mix, Sun Gro Horticulture, Agawam, MA) was thoroughly mixed with nanoplastics suspension prepared in ultra-pure water using a spatula and glass beaker. The volume of the nanoplastics suspension added to the soil was chosen to



1 obtain a volumetric water content of the soil of  $0.25 \text{ cm}^3/\text{cm}^3$ .  
2 The nanoplastic concentrations were chosen such to obtain a final  
3 concentration of ( $0.029 \text{ g/L} = 2.9 \times 10^{-5} \text{ g/cm}^3$  of soil volume).  
4 The plastic-amended soil was packed to a bulk density of  $0.31$   
5  $\text{g/cm}^3$ .

6 For wheat, soil was packed into clay pots. Wheat seeds were  
7 first germinated in Petri dishes with half-strength MS agar media  
8 for two days, and then transferred to the clay pots and grown for  
9 10 days. Wheat roots were then gently pulled from the soil and  
10 washed with half MS strength media to clean roots for confocal  
11 microscopy. The washed plant roots were processed for confocal  
12 imaging in the same way as the agar and hydroponically grown  
13 plants.

14 For *A. thaliana*, we observed that the roots got damaged when  
15 they were removed from soil medium, and we therefore used a  
16 micro-ROC system<sup>17</sup>, which allows the roots to grow without direct  
17 soil contact. This micro-ROC system has been especially developed  
18 to observe root growth by microscopy without having to remove or  
19 clean roots<sup>17</sup>, and has been used in rhizosphere studies<sup>18</sup>. The  
20 micro-ROC system consisted of a  $7 \text{ cm} \times 5 \text{ cm} \times 2 \text{ cm}$   
21 chamber where one side contained a glass plate and a membrane  
22 ( $38 \mu\text{m}$  pore size, #400 Nylon cloth, Gilson Company, Inc., Lewis  
23 Center, OH) in contact with the soil medium (Figure S3). Mesh  
24 and glass slides were attached to the micro-ROC chamber with a  
25 sealant (MarineWeld<sup>TM</sup>, Sulphur Springs, TX). The glass plate of  
26 the micro-ROC system was covered with a black plastic film.

27 The plastic-amended soil was packed into the micro-ROC system  
28 at the same bulk density as for the wheat experiments.  
29 *A. thaliana* plants were grown such that the roots were confined  
30 to the space between the glass slide and the Nylon membrane.  
31 *A. thaliana* seeds were first germinated in Petri dishes with half-  
32 strength MS agar media for two days, and then transferred to the  
33 micro-ROC system and grown for an additional 7 days. The plants  
34 were then removed from the micro-ROCs system by removing the  
35 glass plate and then prepared for confocal microscopy as described  
36 above.

### 40 2.3 Confocal laser scanning microscopy

41 Confocal laser scanning microscopy was performed on a Confocal  
42 Microscope (Leica TCS SP8, Leica Microsystems). Microscopy settings  
43 are listed in Table S1. Confocal images of the nanospheres in agar  
44 medium are shown (Figure S1). The  $40 \text{ nm}$  nanospheres could not  
45 individually be visualized but can be detected as clusters only.  
46 For the  $200 \text{ nm}$  nanospheres, individual particles could be discerned,  
47 but a more pronounced signal was obtained with clustered particles.

48 Before imaging with confocal microscopy, plant roots were  
49 stained by dipping the roots in a propidium iodide (PI) staining  
50 solution ( $0.1 \text{ mg/mL}$ , Sigma-Aldrich) for 30 seconds. A few  
51 drops of half-strength MS solution were placed on a clean  
52 microscopy slide, and then PI stained roots were placed onto the  
53 slide, and then covered with cover slip with minimal disturbance  
54 of the root sections. For both  $40 \text{ nm}$  and  $200 \text{ nm}$  spheres, a  $488$   
55  $\text{nm}$  excitation and a  $500\text{--}550 \text{ nm}$  emission wavelength were used.  
56 To show the propidium iodide stained root cells, an excitation wave-

length of  $561 \text{ nm}$  and an emission wavelength of  $597\text{--}776 \text{ nm}$   
were used. The magnification used was  $10\times$  for wheat and  $40\times$   
for *A. thaliana*. Imaging was done with z-stacks between the top  
and the center of the roots in  $150\text{--}200$  and  $40\text{--}60\mu\text{m}$  increments  
for wheat and *A. thaliana*, respectively.

### 2.4 Scanning electron microscopy (SEM)

Wheat root cross-sections were analyzed with SEM. Wheat roots  
were stored in a formaldehyde, alcohol, acetic acid solution for  
2 weeks, and then cross-sections of  $30 \mu\text{m}$  were prepared with a  
cryostat (Cryocut 1800 Cryostat, Leica) at  $-27^\circ\text{C}$ . Cross-sections  
were then transferred to SEM stubs and 2% paraformaldehyde  
was applied for 2 hours. Cross-sections were then frozen in liquid  
 $\text{N}_2$  and freeze-dried overnight. Samples were finally gold-coated  
and analyzed by SEM (FEI Quanta 200F). Per treatment, three  
plants were used for SEM, and for each root 10 to 12 cross-sections  
were analyzed.

### 2.5 Plant biomass measurements

To determine the effects of plastic particles on plant growth,  
*A. thaliana* (20 days grown) and wheat plants (10 days grown)  
in agar and hydroponics were processed for biomass measurements  
by drying leaves and roots separately. Dry biomass was determined  
after drying the plants in an oven at  $70^\circ$  for three days. Six  
plants for *A. thaliana* and three plants for wheat were grown in  
Magenta boxes per treatment and the experiments replicated three  
times (Figure S4).

### 2.6 Reactive Oxygen Species (ROS) measurements

To measure the hydrogen peroxide and superoxide accumulation  
in plant roots and leaves, the protocol developed by Bittner et al.<sup>19</sup>  
was followed. Seedlings (7 days old) and leaves (20 days old)  
from *A. thaliana* were processed for ROS measurements. First,  
*A. thaliana* seedlings in hydroponics were stained overnight with  
DAB (3,3-Diaminobenzidine) for hydrogen peroxide accumulation  
and NBT (Nitroblue Tetrazolium) for superoxide accumulation.  
After staining, stained seedlings and leaves were washed with a  
de-staining solution consisting of ethanol, acetic acid, and glycerol  
in a hot water bath at  $60^\circ\text{C}$ . After the de-staining procedure when  
the plants looked almost white, the plants were imaged with a  
fluorescence microscope (LEICA M205 FA, Leica Microsystems).

The images obtained from the fluorescence microscope were  
analyzed with ImageJ<sup>20</sup>. The original color images (RGB format)  
were converted to a grey scale with a 32-bit format. These black  
and white pictures were then used to quantify the area of the  
original coloration (red for DAB and blue for NBT, respectively)<sup>19</sup>.

### 2.7 Quality assurance and quality control

All the materials used for plant growth experiments were  
sterilized to ensure no microbial growth in growth media and  
plant roots themselves. Sterilization was done by autoclaving  
the growth media at  $121^\circ\text{C}$  for 50 minutes, whereas the plant  
seeds were sterilized by 20% bleach and Triton X-100, and ethanol as

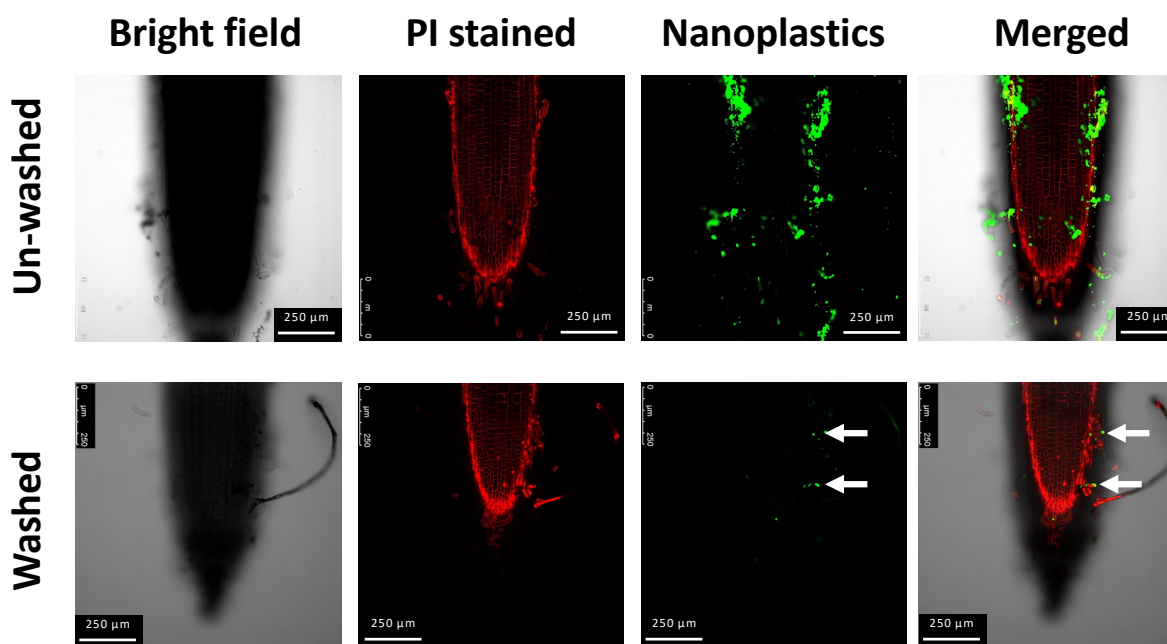


Fig. 1 Confocal images of wheat roots (un-washed versus washed) grown in hydroponic solution with 200 nm carboxylate-modified polystyrene spheres. Arrow indicate nanospheres attached to the root surface after washing. PI: propidium iodide.

mentioned in the agar and hydroponics methods section. Seed sterilization and all sample processing tasks were done in the laminar flow hood to limit ambient plastics contamination. Control treatments with no plastics were included along with the plastic treatments for all experiments. For washing the seedlings before confocal imaging, autoclaved half strength MS solutions were used.

## 2.8 Statistical analysis

Statistical analysis was done in RStudio to test for differences in shoot and root biomass of the different treatments. ANOVA and Tukey HSD tests were used to compare means of different treatments and to determine the  $p$ -values. Statistical significance was considered at the  $p < 0.05$  level.

## 3 Results and Discussion

In the following, we will discuss the associations of the nanospheres with the wheat and *A. thaliana* roots for agar, hydroponics, and soil media. We will then compare the effects of nanosphere size and surface charge. Finally, we will discuss the impacts of the nanospheres on biomass and plant stress.

### 3.1 Washed versus non-washed roots

The gentle washing by immersing the roots in clean half MS solution removed a substantial amount of nanospheres associated with the roots (Figure 1). This indicates that a large portion of the nanospheres were loosely attached and not internalized into the root tissue. A small fraction of the spheres, however, remained attached to the root epidermis after washing.

### 3.2 Nanoplastics association with plants grown in agar medium

**Wheat:** Confocal images of wheat roots indicate that the different types of nanospheres visible in the images were located at the surface of the roots (Figure 2, left and Figure S5). No nanosphere fluorescence could be detected inside the root tissue, as evidenced when examining the  $z$ -stacks, which indicate fluorescence along root hairs and the perimeter of the roots only (Figure S5).

Scanning electron microscopy images, however, indicate that the 40 nm carboxylate-modified spheres could penetrate into the wheat roots (Figure 3, left). The 40 nm spheres were detected in the vascular system of the roots, but there was no evidence for the presence of the 200 nm carboxylate- and amino-modified spheres in either the cortex or the vascular tissue. Only a few 40-nm spheres were detected in the vascular tissue, which explains why the confocal images did not show these spheres, as the confocal microscope resolution was not sufficient to resolve individual 40-nm spheres.

**Arabidopsis thaliana:** The confocal images of agar grown *A. thaliana* indicate no distinct fluorescence inside the roots (Figure 2, right). The nanoplastics were adhered to the outer surface of the roots in aggregates. The  $z$ -stack images also show no conclusive evidence of nanoplastics entry into the root's interior (Figure S6).

Taylor et al.<sup>15</sup> also did not find evidence for root entry of 40 nm polystyrene nanoplastics for agar grown *A. thaliana*; confocal imaging only indicated that nanoplastics attached to the root cap cells. On the other hand, Parkinson et al.<sup>21</sup>, also using confocal imaging, found that negatively charged 50 nm polystyrene spheres were taken up by agar grown *A. thaliana*; however, the concentrations of the polystyrene spheres used was about 35

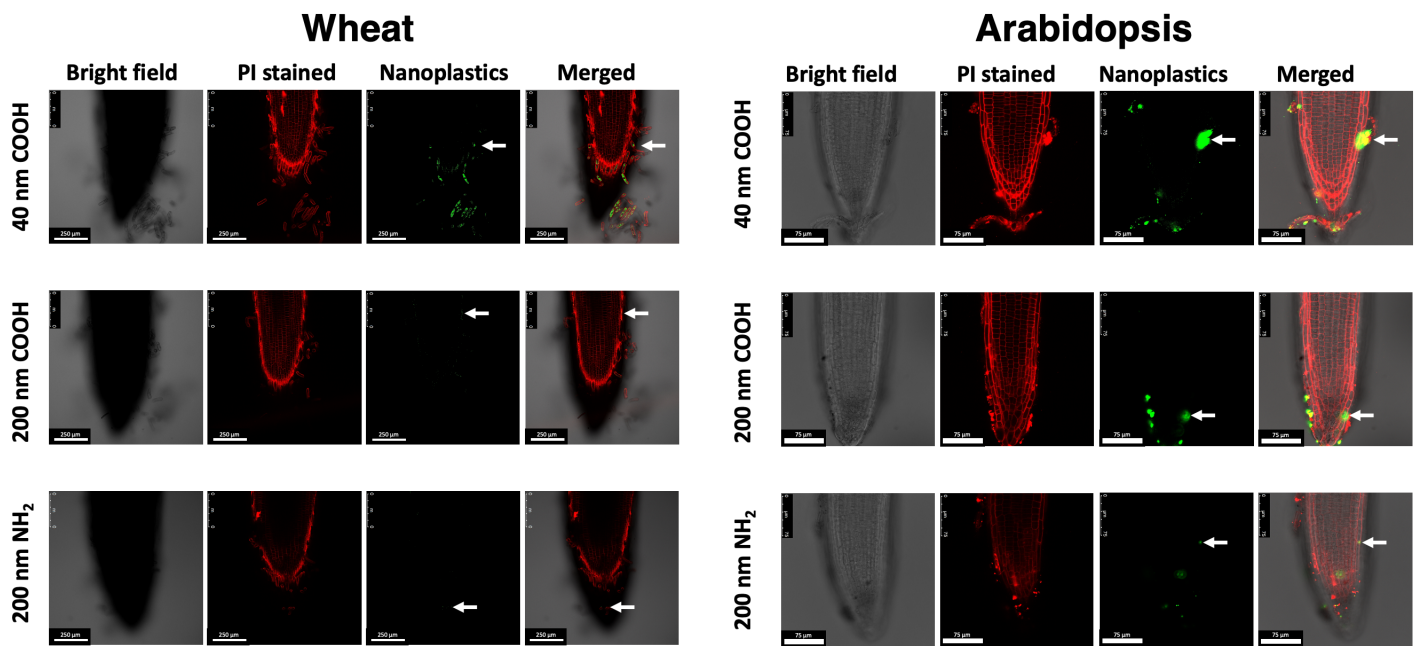


Fig. 2 Wheat (left) and *Arabidopsis thaliana* (right) in agar medium: Confocal images of roots for 40 nm carboxylate-modified polystyrene nanospheres, 200 nm carboxylate-modified polystyrene nanospheres, and 200 nm amino-modified polystyrene nanospheres. The images were focused about 225  $\mu\text{m}$  above the center of the root. Arrows indicate nanospheres attached to the root cap cells. PI: propidium iodide.

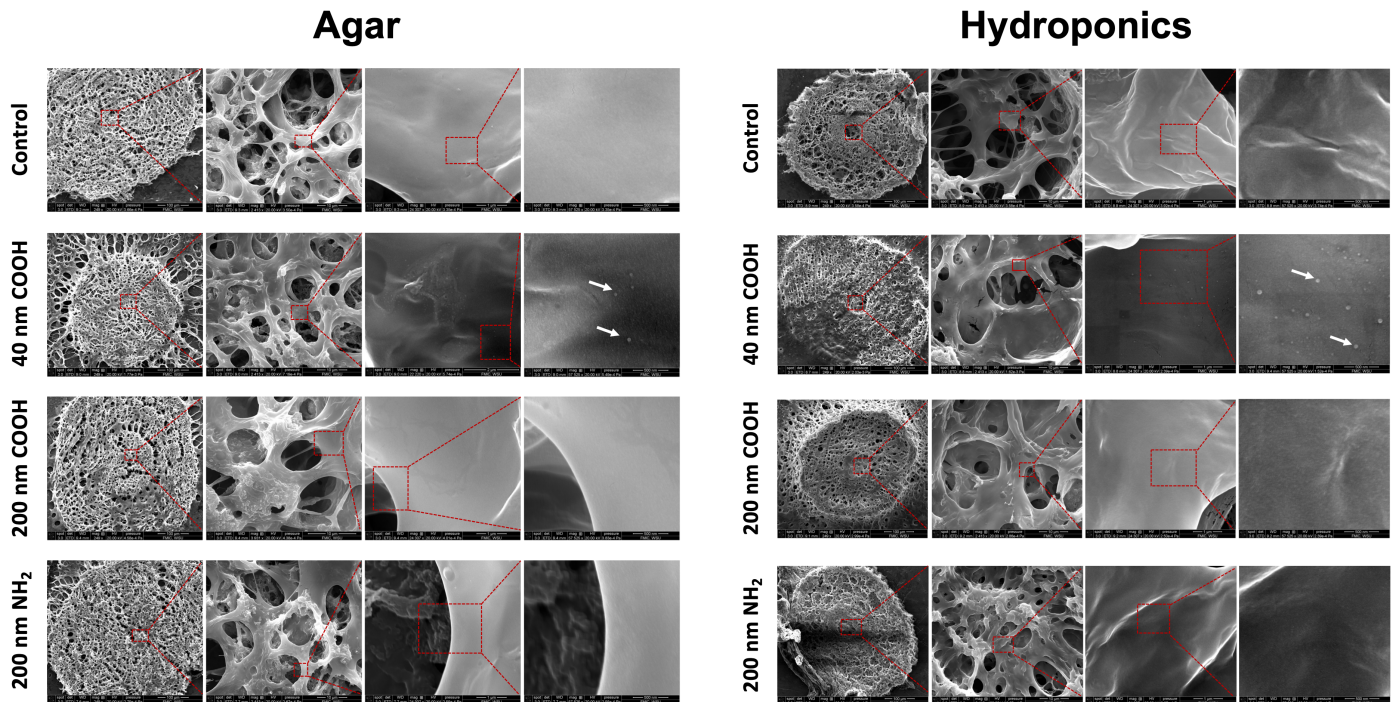


Fig. 3 Scanning electron microscopy images of wheat root cross-sections in agar (left) and hydroponics (right): Control (no spheres), 40 nm carboxylate-modified polystyrene nanospheres, 200 nm carboxylate-modified polystyrene nanospheres, and 200 nm amino-modified polystyrene nanospheres. Images show different magnifications as indicated by the red boxes. Cross-sections shown were taken about 1 mm from the root tip. Arrows indicate nanospheres inside the vascular system, detected only for the 40 nm spheres.



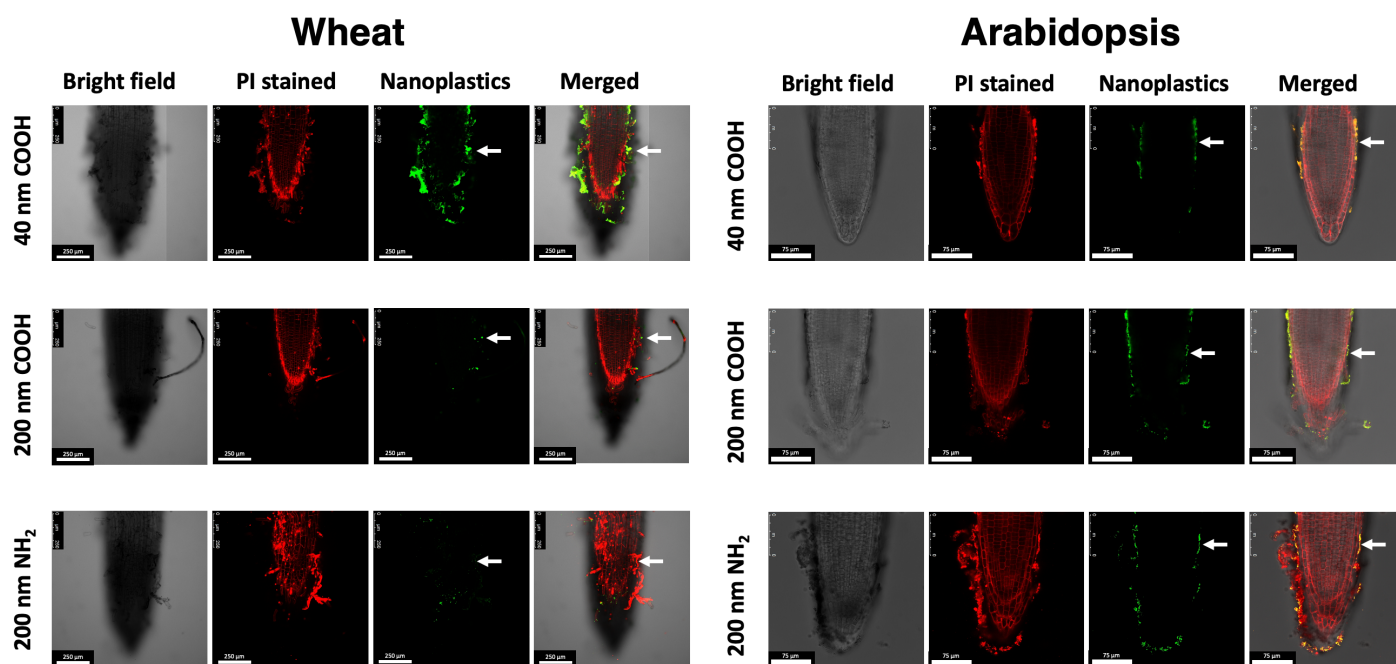


Fig. 4 Wheat (left) and *Arabidopsis thaliana* (right) in hydroponics medium: Confocal images of roots for 40 nm carboxylate-modified polystyrene nanospheres, 200 nm carboxylate-modified polystyrene nanospheres, and 200 nm amino-modified polystyrene nanospheres. The images were focused about 225  $\mu\text{m}$  above the center of the root. Arrows indicate nanospheres attached to the root cap cells. PI: propidium iodide.

times larger.

### 3.3 Nanoplastics association with plants grown in hydroponic system

**Wheat:** In hydroponic solutions, the nanospheres were associated mainly at the surface, i.e., epidermis, of the wheat roots (Figure 4, left and Figure S7), irrespective of size or surface charge. Confocal images of wheat root tips did not reveal conclusively whether spheres were taken up into the interior of the roots. The  $z$ -stack images rather indicate that the spheres accumulated at the root surface as the fluorescence of the spheres was mostly confined to outside cross-section in each  $z$ -stack. As the focal plane of the microscope was moved from top to the center of the root, the fluorescent signal of the nanospheres remained mainly at the outline of the root (Figure S7).

The strongest fluorescent signal from the nanospheres was obtained with the 40 nm nanospheres, a much weaker signal was detected for the 200 nm spheres (Figure 4, left), indicating that the 40 nm nanospheres were more strongly attached to the root surface than the 200 nm spheres, which could more readily be washed off by gentle rinsing of the roots (Figure 1).

The SEM images of the wheat root cross-sections are shown in Figure 3 (right). Spheres were detected inside the roots for the 40 nm polystyrene spheres treatment; no 200 nm spheres were detected inside the root cross-sections. We detected the 40 nm spheres in the vascular system, indicating that the 40 nm spheres were able to penetrate into the center of the roots and were able to pass through the Casparian strip.

**Arabidopsis thaliana:** The confocal images indicate that the

nanospheres were mostly confined to the exterior of the roots, with the fluorescence of the spheres only visible at the outermost cell layers, i.e., the epidermis (Figure 4, right). This was confirmed by the  $z$ -stack images, which show that the sphere fluorescence remained at the outline of the root cross-sections as the focal plane of the microscope moved through the  $z$ -direction of the root tip (Figure S8).

For the amino-modified nanospheres, we observed extensive mucilage around the root tips (Figure 4, right and Figure S8). The nanospheres were mainly located in this mucilage layer. Considerably more fluorescence around the roots was observed for the hydroponics system as compared to the agar system.

### 3.4 Nanoplastics association with plants grown in soil

For soil grown wheat seedlings, the fluorescence of the spheres was considerably lower as compared to agar and hydroponics systems, and fewer nanospheres were attached to root caps (Figure 5, left and Figure S9). This is because, in the presence of soil, the exposure of plant roots to nanoplastics is limited. Plant roots can access readily available nanoplastics in soil pore water, whereas nanoplastics sorbed to soil particles and organic matter are only available after desorption<sup>22</sup> or root interception. In the case of *A. thaliana*, where the roots were not directly in contact with the soil particles, the nanospheres were still accessible to plant roots as we observed fluorescent nanospheres attached to the root surfaces (Figure 5, right). However, the fluorescence was considerably less pronounced than in agar and hydroponics systems.

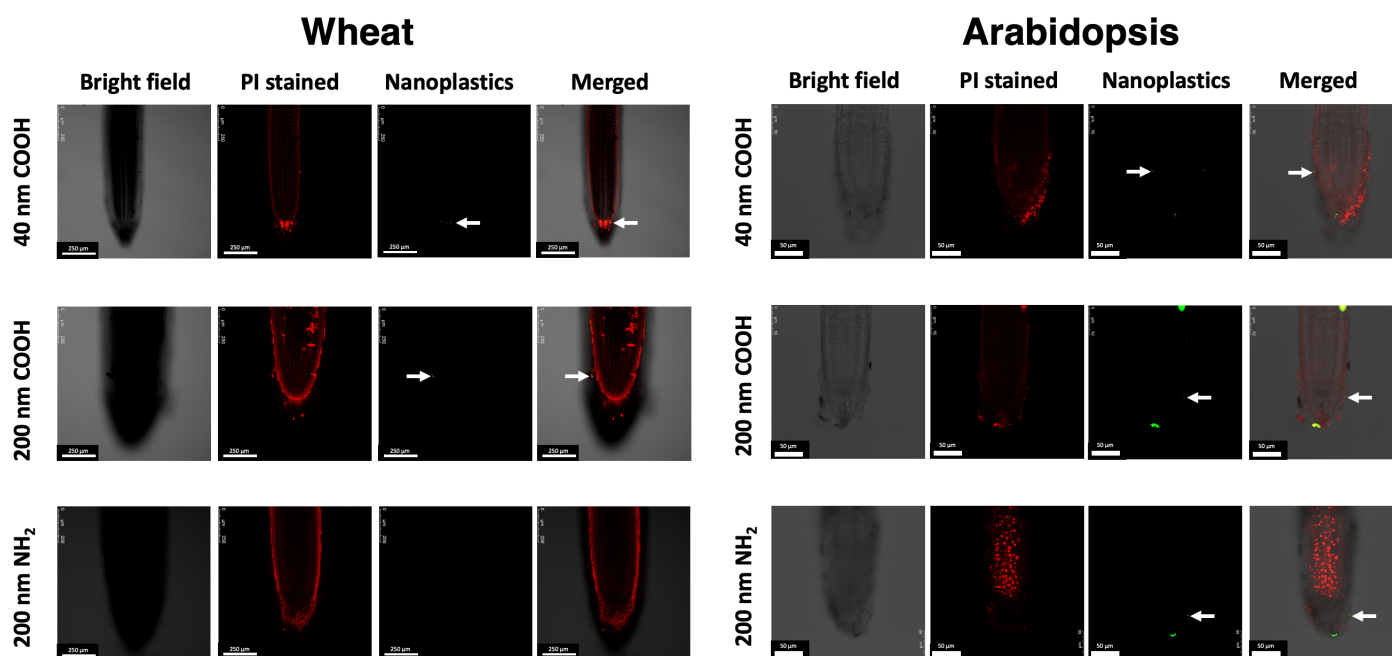


Fig. 5 Wheat (left) and *Arabidopsis thaliana* (right) in soil medium: Confocal images of roots for 40 nm carboxylate-modified polystyrene nanospheres, 200 nm carboxylate-modified polystyrene nanospheres, and 200 nm amino-modified polystyrene nanospheres. The images were focused about 225  $\mu\text{m}$  above the center of the root. Arrows indicate nanospheres attached to the root cap cells. PI: propidium iodide.

### 3.5 Mechanisms and pathways of nanoplastic uptake by roots

A higher number of nanospheres were associated with plant roots grown in hydroponics as compared to agar and soil. Hydroponics systems offer more opportunity for plant roots to be exposed to nanoparticles because the particles are more mobile and therefore more readily bioavailable than in agar and soil<sup>23,24</sup>. In agar, nanospheres are immobile and can only interact with plant roots when the roots make direct contact with the nanospheres, so the probability of nanospheres-root contact is much smaller in an agar system as compared to a hydroponics system.

In soil, the mobility of nanospheres depends on various factors, such as the size and surface charge of the spheres, and the tortuosity and connectivity of the flow pathways. Furthermore, positively charged nanospheres will be attached to the generally negatively charged soil particles by electrostatic forces, and will therefore only interact with roots through direct contact when a root intercepts a nanosphere during root growth. Negatively charged nanospheres, on the other hand, can be mobile and can move to the root surface via diffusion and convective water flow driven by transpiration. Nonetheless, attachment of negatively charged nanospheres still can occur through pore straining, water film straining, wedging, attachment to the air-water interface or the air-water solid triple point<sup>4</sup>. These mechanisms make nanospheres in soils generally less mobile than in hydroponics systems<sup>25</sup>.

Further, plants grown in hydroponics systems have higher transpiration rates which facilitates nanoplastics uptake as compared to soils<sup>23</sup>. Li et al.<sup>5</sup> observed higher uptake and toxicity of 200

nm polystyrene nanoplastics by plant roots grown in hydroponics whereas no uptake was seen in soil grown plant roots. In our study, we did not observe intracellular accumulations in hydroponics, agar, or soil; however, extracellular accumulation and attachment of nanospheres was higher in hydroponics as compared to soils likely due to higher transpiration rate and higher mobility of nanospheres in hydroponics systems.

We did not observe a notable difference between differently charged polystyrene nanospheres, i.e., 200 nm COOH-modified (negative,  $-21.4 \pm 1.8$  mV) and 200 nm  $\text{NH}_2$ -modified (positive,  $-7.8 \pm 4.1$  mV) (Table 1), in terms of their association with plant roots. Sun et al.<sup>6</sup> showed higher uptake of negatively charged 200 nm nanospheres than of positively charged ones. However, in our study, confocal and electron microscopy analysis did not show visual differences in the association of differently charged nanospheres. This contradictory result between these two studies may be due to higher surface charges of the nanospheres used in the Sun et al.<sup>6</sup> study, where the carboxylate-modified spheres had a zeta potential of  $-53.7$  mV (vs  $-21.4$  mV in our study) and the amine-modified spheres had a zeta potential of  $+28.1$  mV (vs  $+7.8$  mV in our study).

We observed that higher numbers of small sized (40 nm) nanospheres were attached to root cap cells as compared to bigger nanospheres (200 nm) (Figures 2 and 4), and only the 40 nm spheres were detected in the interior of the stele by SEM. Smaller sized nanospheres are more prone to root uptake because of size exclusion limits and chemical and physiological barriers in both the symplastic and apoplastic uptake pathways<sup>10,26,27</sup>. Data compiled in a recent review<sup>28</sup> suggest that only particles of size



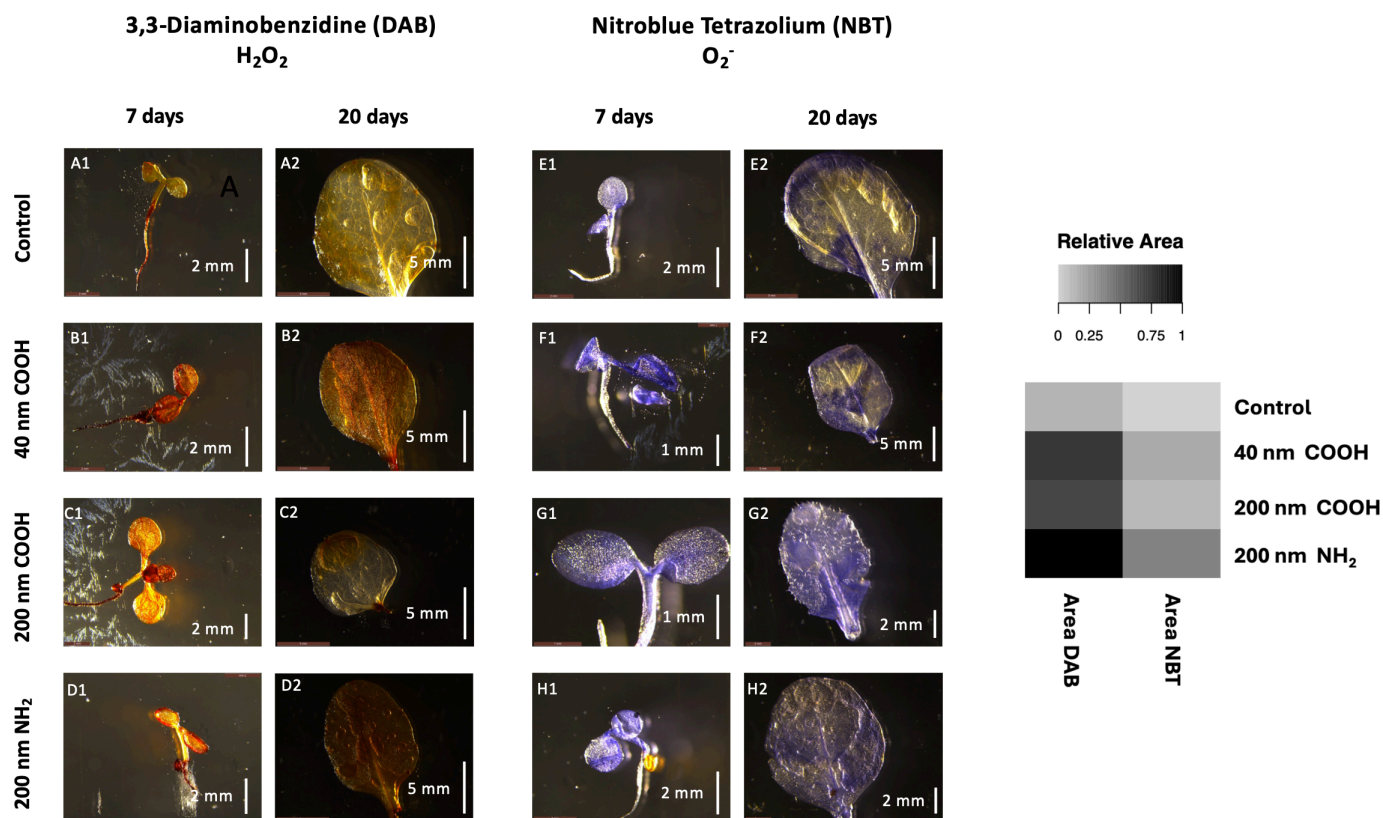


Fig. 6 Fluorescent images (left) and heatmap (right) showing reactive oxygen species (ROS) accumulation in *Arabidopsis thaliana* in hydroponics. Hydrogen peroxide accumulation is shown by red coloration in 7 days grown whole seedlings and in 20 days grown leaves (A,B,C,D). Superoxide accumulation is shown by blue coloration in 7 days grown whole seedlings and in 20 days grown leaves (E,F,G,H). Heatmap shows ROS accumulation on 20 days grown *A. thaliana* leaves as quantified using ImageJ based on area of brown (DAB) and blue (NBT) coloration. The darker the shading, the greater is the area of coloration, indicating greater ROS accumulation. The statistical differences among the different treatments are listed in Table S3.

of <50 nm can be taken up by roots into the vascular system, whereas particles of size of >100 nm remain on the epidermis. The 40 nm nanospheres in our experiments were likely absorbed by the roots via the apoplastic pathway, and then could penetrate the Casparian strip to enter into the vascular system, as evidenced by the detection of the nanospheres in the stele by SEM.

### 3.6 Effects of nanoplastics on plant biomass

Wheat and *A. thaliana* plants grown in agar and hydroponics systems with nanoplastics generally showed reduced biomass compared to the control (Figure S4 and Figure S10). The root-to-shoot biomass ratio was also higher for the control than for the nanoplastic treatments (Table S2), indicating that the nanoplastics did interfere with root growth. Sun et al.<sup>6</sup> also observed a reduction in root length when *A. thaliana* was exposed to polystyrene nanospheres at three different concentrations (10, 50, and 100  $\mu\text{g}/\text{mL}$ ) in half strength MS agar media.

The largest reduction in plant biomass was observed for both wheat and *A. thaliana* for the 40 nm nanospheres in hydroponics systems (Figure S10 and Table S2). This reduction in biomass in hydroponics can be explained by more frequent interactions of plant roots with nanoplastics because the nanoplastic particles

can move freely, exposing the plant roots to more nanoplastics than in agar.

In addition, the root and shoot biomass of *A. thaliana* exposed to 40 nm carboxylate-modified and 200 nm amino-modified spheres was significantly lower than that of *A. thaliana* exposed to 200 nm carboxylate-modified spheres. Some of the 40 nm carboxylate-modified spheres were taken up into the vascular tissue of the roots, likely causing the observed reduction in biomass. The 200 nm amino-modified spheres were not detected in the vascular tissue and, like the 200 nm carboxylate-modified spheres, remained concentrated along the epidermis cells. However, due to their positive charge, the amino-modified spheres interact more strongly with the root cells, and thereby can cause more harm to root growth. This is corroborated with the observed higher levels of ROS induced by the amino-modified spheres as discussed below.

### 3.7 Effect of nanoplastics on reactive oxygen (ROS) generation

To evaluate whether the reduced biomass of *A. thaliana* in hydroponics was associated with an increased concentration of ROS, we assessed the amount of ROS with DAB (3,3-diaminobenzidine)

1 and NBT (nitrioblu tetrazolium). We observed ROS accumu-  
2 lation in *A. thaliana* seedlings and leaves, as indicated by red  
3 ( $\text{H}_2\text{O}_2$ ) and blue ( $\text{O}_2^-$ ) coloration (Figure 6, left). Qualitatively,  
4 nanosphere treatments produced higher ROS accumulation com-  
5 pared to control plants, as indicated by the more intensive col-  
6 oration (Figure 6, left). Semi-quantitative analysis showed that  
7 the 200 nm amino-modified spheres produced more ROS accumu-  
8 lation as compared to 40 nm and 200 nm carboxylate-modified  
9 spheres (Figure 6, right).

10 We also observed effects of nanoparticle size and surface charge  
11 on ROS accumulation: negatively charged 40 nm and positively  
12 charged 200 nm spheres yielded higher ROS accumulation as  
13 compared to negatively charged 200 nm spheres (Figure 6, right).  
14 Sun et al.<sup>6</sup> also reported higher  $\text{H}_2\text{O}_2$  accumulation in *A. thaliana*  
15 exposed to positively charged polystyrene nanospheres compared  
16 to negatively charged nanospheres. In other studies on duck-  
17 weed and dandelion exposed to nanospheres, the effect of pos-  
18 itively charged nanospheres on ROS accumulation was more pro-  
19 nounced than those of negatively charged nanospheres<sup>29,30</sup>. Pos-  
20 itively charged nanospheres exhibit a tendency to undergo het-  
21 eroaggregation when interacting with negatively charged mu-  
22 cilages and exudates excreted by plant roots<sup>6,31</sup>. This phe-  
23 nomenon of heteroaggregation can lead to the obstruction of root  
24 pores, thereby reducing the uptake of water and nutrients by  
25 plant roots. Consequently, this obstruction may facilitate the gen-  
26 eration of ROS. The size-specific effects observed are attributed  
27 to the high surface area of small-sized nanospheres, which pro-  
28 mote increased interaction with plant roots and subsequently con-  
29 tribute to the accumulation of ROS.

30 Generally, plants produce ROS as a response to stress, such as  
31 exposure to pathogens<sup>32,33</sup>. The elevated level of ROS when  
32 *A. thaliana* was exposed to plastic nanospheres indicates that  
33 the plants recognized the plastic nanospheres as a stressor. If  
34 ROS levels get too high, then oxidative damage to plant cells  
35 can occur<sup>34,35</sup> and plant growth and yield can be negatively im-  
36 pacted<sup>36</sup>. In our experiments, we observed elevated levels of  
37 ROS for all plastic treatments, but we did not observe visual cell  
38 damage or chlorosis. However, for the negatively charged 40 nm  
39 and positively charged 200 nm spheres we observed a reduced  
40 shoot and root biomass, indicating that the ROS levels were high  
41 enough to cause a phenomenological response, likely a result of  
42 reduced photosynthetic activity<sup>34,37</sup>.

## 45 4 Implications

46 Micro- and nanoplastics in soil can associate with plant roots  
47 in soil, with small nanoplastics (40 nm in our study) taken up  
48 by plant roots and translocated into the vascular system of the  
49 plants. Larger plastic particles (200 nm in our study) could not  
50 penetrate into the vascular system, but nonetheless could attach  
51 to the root epidermis. Nanoplastics can have negative impacts on  
52 root growth, impacting root and shoot biomass, indicating long-  
53 term environmental fate and ecological consequences of plastic  
54 particles.

55 However, most evidence about plant uptake of micro- and  
56 nanoplastics stems from experiments with model plastic beads,  
57 i.e., polystyrene spheres, and with plants grown in hydroponics

or agar systems. While such studies help to elucidate the mecha-  
nisms of plastic uptake by plant roots and show that plastic par-  
ticles can be internalized by roots, we can not conclude from  
such studies that plastic particles in field soils are indeed taken  
up by plants also. In our study, we found less plant uptake of  
nanospheres in soils compared to agar and hydroponics systems,  
indicating that plastic uptake in field soils is less pertinent than  
in agar or hydroponics systems. Plastics found in field soils come  
in many different and irregular shapes, have considerable surface  
roughness, and can be attached to soil particles, making them  
less mobile<sup>4</sup>. These attributes make environmentally weathered  
plastics in soils less plant available compared to model spheres in  
hydroponics or agar systems. Further, environmentally relevant  
plastic concentrations in soils are often much lower than those  
used in experimental studies<sup>38</sup>, making plant uptake of plastic  
particles less likely.

Nonetheless, plastic pollution of soils leads to the possibility of  
contamination of plant-based products with micro- and nanoplas-  
tics and subsequent human exposure to micro- and nanoplastics  
through food consumption. Recent evidence of the existence of  
micro- and nanoparticles in the human blood stream<sup>39–42</sup> shows  
that micro- and nanoparticles reach places where they should not  
be. The human health impacts of the consumption of micro- and  
nanoparticles still needs to be evaluated, and steps should be  
taken to limit direct exposure of humans to plastic by consump-  
tion of plastic-contaminated food.

## Author Contributions

Conceptualization: Markus Flury, Karen Sanguinet, Carolyn  
Pearce, Kaushik Adhikari

Roles/Writing—original draft: Kaushik Adhikari, Markus Flury

Methodology: Kaushik Adhikari, Markus Flury, Karen Sanguinet,  
Carolyn Pearce

Formal analysis: Kaushik Adhikari, Markus Flury, Karen San-  
guinet

Visualization: Kaushik Adhikari

Writing—review & editing: all co-authors

## Conflicts of interest

There are no conflicts to declare.

## Acknowledgements

This work was supported by Agroecosystems grant 2020-67019-  
31149/1022234 from the USDA National Institute of Food  
and Agriculture. Funding was further provided by Northwest  
Biosolids, by King County, Department of Natural Resources and  
Parks, and by USDA/NIFA through Hatch project 1014527 and  
W4188 Multi-State Project. We thank Bhabesh Borphukan for  
the help with ROS measurements. We thank the WSU Franceschi  
Microscopy and Imaging Center for access to their facility and Va-  
lerie Lynch-Holm for help with the use of the electron microscope.

## Notes and references

- 1 M. Bläsing and W. Amelung, Plastics in soil: Analytical meth-  
ods and possible sources, *Sci. Total Environ.*, 2018, **612**, 422–  
435.

- 1  
2 R. R. Hurley and L. Nizzetto, Fate and occurrence of micro  
3 (nano) p lastics in soils: Knowledge gaps and possible risks,  
4 *Current Opinion in Environmental Science & Health*, 2018, **1**,  
5 6–11.
- 6 3 A. F. Astner, A. B. Gillmore, Y. Yu, M. Flury, J. M. DeBruyn,  
7 S. M. Schaeffer and D. G. Hayes, Formation, Behavior, Prop-  
8 erties and Impact of Micro- and Nanoplastics on Agricultural  
9 Soil Ecosystems (A Review), *NanoImpact*, 2023, **31**, 100474,  
10 doi:10.1016/j.impact.2023.100474.
- 11 4 Y. Yu and M. Flury, Current understanding of subsurface trans-  
12 port of micro- and nanoplastics in soil, *Vadose Zone J.*, 2021,  
13 **20**, e20108, doi:10.1002/vzj2.20108.
- 14 5 L. Li, Y. Luo, R. Li, Q. Zhou, W. J. G. M. Peijnenburg, N. Yin,  
15 J. Yang, C. Tu and Y. Zhang, Effective uptake of submicrome-  
16 tre plastics by crop plants via a crack-entry mode, *Nature Sus-  
17 tainability*, 2020, **3**, 929–937.
- 18 6 X.-D. Sun, X.-Z. Yuan, Y. Jia, L.-J. Feng, F.-P. Zhu, S.-S. Dong,  
19 J. Liu, X. Kong, H. Tian, J.-L. Duan, Z. Ding, S.-G. Wang, and  
20 B. Xing, Differentially charged nanoplastics demonstrate dis-  
21 tinct accumulation in *Arabidopsis thaliana*, *Nature Nanotech-  
22 nology*, 2020, **15**, 755–760.
- 23 7 A. P. de Luque, Interaction of Nanomaterials with Plants:  
24 What Do We Need for Real Applications in Agriculture?,  
25 *Frontiers in Environmental Science*, 2017, **5**, 12, doi:  
26 10.3389/fenvs.2017.00012.
- 27 8 I. Azeem, M. Adeel, M. A. Ahmad, N. Shakoor, G. D.  
28 Jiangcuo, K. Azeem, M. Ishfaq, A. Shakoor, M. Ayaz, M. Xu  
29 *et al.*, Uptake and Accumulation of Nano/Microplastics in  
30 Plants: A Critical Review, *Nanomaterials*, 2021, **11**, 2935,  
31 doi.org/10.3390/nano11112935.
- 32 9 A. Avellan, F. Schwab, A. Masion, P. Chaurand, D. Borsch-  
33 neck, V. Vidal, J. Rose, C. Santaelle and C. Levard, Nanopar-  
34 ticle Uptake in Plants: Gold Nanomaterial Localized in Roots  
35 of *Arabidopsis thaliana* by X-ray Computed Nanotomography  
36 and Hyperspectral Imaging, *Environmental Science & Technol-  
37 ogy*, 2017, **51**, 8682–8691.
- 38 10 Y. Dong, M. Gao, W. Qiu and Z. Song, Uptake of microplas-  
39 tics by carrots in presence of As (III): Combined toxic ef-  
40 fects, *Journal of Hazardous Materials*, 2021, **411**, 125055,  
41 doi:10.1016/j.jhazmat.2021.125055.
- 42 11 C. Spanò, S. Muccifora, M. R. Castiglione, L. Bellani, S. Bot-  
43 tega and L. Giorgetti, Polystyrene nanoplastics affect seed  
44 germination, cell biology and physiology of rice seedlings in-  
45 short term treatments: Evidence of their internalization and  
46 translocation, *Plant Physiology and Biochemistry*, 2022, **172**,  
47 158–166.
- 48 12 H. Sahai, M. J. M. Bueno, M. del Mar Gómez-Ramos,  
49 A. R. Fernández-Alba and M. D. Hernando, Quantifica-  
50 tion of nanoplastic uptake and distribution in the root,  
51 stem and leaves of the edible herb *Lepidium sativum*,  
52 *Science of the Total Environment*, 2024, **912**, 168903,  
53 doi.org/10.1016/j.scitotenv.2023.168903.
- 54 13 S. Rong, S. Wang, H. Liu, Y. Li, J. Huang, W. Wang,  
55 B. Han, S. Su and W. Liu, Evidence for the transporta-  
56 tion of aggregated microplastics in the symplast pathway  
57 of oilseed rape roots and their impact on plant growth,  
58 *Science of the Total Environment*, 2024, **912**, 169419,  
59 doi:10.1016/j.scitotenv.2023.169419.
- 60 14 C. Sun, X. Yang, Q. Gu, G. Jiang, L. Shen, J. Zhou, L. Li,  
H. Chen, G. Zhang and Y. Zhang, Comprehensive analy-  
sis of nanoplastic effects on growth phenotype, nanoplas-  
tic accumulation, oxidative stress response, gene expression,  
and metabolite accumulation in multiple strawberry culti-  
vars, *Science of the Total Environment*, 2023, **897**, 165432,  
doi.org/10.1016/j.scitotenv.2023.165432.
- 15 S. E. Taylor, C. I. Pearce, K. A. Sanguinet, D. Hu, W. B. Chrisler,  
Y.-M. Kim, Z. Wang and M. Flury, Polystyrene nano-and mi-  
croplastic accumulation at *Arabidopsis* and wheat root cap  
cells, but no evidence for uptake into roots, *Environmental  
Science: Nano*, 2020, **7**, 1942–1953.
- 16 T. Murashige and F. Skoog, A revised medium for rapid  
growth and bio assays with Tobacco tissue cultures, *Physiolo-  
gia Plantarum*, 1962, **15**, 437–497.
- 17 P. T. Dinh, M. Knoblauch and A. A. Elling, Nondestructive  
imaging of plant-parasitic nematode development and host  
response to nematode pathogenesis, *Phytopathology*, 2014,  
**104**, 497–506.
- 18 R. Kooliyottill, L.-M. Dandurand, B. N. Govindan and  
G. R. Knudsen, Microscopy method to compare cyst nematode  
infection of different plant species, *Advances in Bioscience and  
Biotechnology*, 2016, **7**, 311–318.
- 19 A. Bittner, T. Griebel, J. van Buer, I. Juszczak-Debosz and  
M. Baier, *Plant Cold Acclimation: Methods and Protocols*, Hu-  
mana Press, Springer, New York, 2020.
- 20 NIH, *ImageJ*, A public domain Java image processing  
program from National Institute of Healths, on-line at  
<http://rsb.info.nih.gov/ij>, accessed in March 2024, 2024.
- 21 S. J. Parkinson, S. Tungsirisurp, C. Joshi, B. L. Richmond,  
M. L. Gifford, A. Sikder, I. Lynch, R. K. O'Reilly and R. M.  
Napier, Polymer nanoparticles pass the plant interface, *Nature  
Communications*, 2022, **13**, 7385, doi.org/10.1038/s41467-  
022-35066-y.
- 22 S. Maity, R. Guchhait, M. B. Sarkar and K. Pramanick, Occur-  
rence and distribution of micro/nanoplastics in soils and their  
phytotoxic effects: A review, *Plant, Cell & Environment*, 2022,  
**45**, 1011–1028.
- 23 D. Savvas and N. Gruda, Application of soilless culture tech-  
nologies in the modern greenhouse industry — A review, *Eu-  
ropean Journal of Horticultural Science*, 2018, **83**, 280–293.
- 24 P. Zhou, L. Wang, J. Gao, Y. Jiang, M. Adeel and D. Hou,  
Nanoplastic–plant interaction and implications for soil health,  
*Soil Use and Management*, 2023, **39**, 13–42.
- 25 L. Wang, W.-M. Wu, N. S. Bolan, D. C. W. Tsang,  
Y. Li, M. Qin and D. Hou, Environmental fate, toxic-  
ity and risk management strategies of nanoplastics in  
the environment: Current status and future perspec-  
tives, *Journal of Hazardous Materials*, 2021, **401**, 123415,  
doi.org/10.1016/j.jhazmat.2020.123415.
- 26 Z. Li, Q. Li, R. Li, J. Zhou and G. Wang, The distribution and  
impact of polystyrene nanoplastics on cucumber plants, *Envi-*

- ronmental Science and Pollution Research, 2021, **28**, 16042–16053.
- 27 Z. Yu, X. Xu, L. Guo, R. Jin and Y. Lu, Uptake and transport of micro/nanoplastics in terrestrial plants: Detection, mechanisms, and influencing factors, *Science of the Total Environment*, 2024, **907**, 168155, doi.org/10.1016/j.scitotenv.2023.168155.
- 28 L. Stolte Bezerra Lisboa Oliveira and K. D. Ristroph, Critical Review: Uptake and Translocation of Organic Nanodelivery Vehicles in Plants, *Environmental Science & Technology*, 2024, **58**, 5646–5669.
- 29 F. Xiao, L.-J. Feng, X.-D. Sun, Y. Wang, Z.-W. Wang, F.-P. Zhu and X.-Z. Yuan, Do polystyrene nanoplastics have similar effects on duckweed (*Lemna minor* L.) at environmentally relevant and observed-effect concentrations?, *Environmental Science & Technology*, 2022, **56**, 4071–4079.
- 30 M. Gao, L. Bai, X. Li, S. Wang and Z. Song, Effects of polystyrene nanoplastics on lead toxicity in dandelion seedlings, *Environmental Pollution*, 2022, **306**, 119349, doi.org/10.1016/j.envpol.2022.119349.
- 31 J. Yang, H. Duan, X. Wang, H. Zhang and Z. Zhang, Effects of rice root exudates on aggregation, dissolution and bioaccumulation of differently-charged Ag nanoparticles, *RSC Advances*, 2022, **12**, 9435–9444.
- 32 K. Apel and H. Hirt, Reactive Oxygen Species: Metabolism, Oxidative Stress, and Signal Transduction, *Annu. Rev. Plant Biol.*, 2004, **55**, 373–399.
- 33 R. Mittler, S. I. Zandalinas, Y. Fichman and F. V. Breusegem, Reactive oxygen species signalling in plant stress responses, *Nature Reviews Molecular Cell Biology*, 2022, **23**, 633–679.
- 34 S. S. Gill and N. Tuteja, Reactive oxygen species and antioxidant machinery in abiotic stress tolerance in crop plants, *Plant Physiology Biochemistry*, 2020, **48**, 909e930, doi.org/10.1016/j.plaphy.2010.08.016.
- 35 B. Castro, M. Citterico, S. Kimura, D. M. Stevens, M. Wrzaczek and G. Coaker, Stress-induced ROS compartmentalization, perception, and signaling, *Nature Plants*, 2021, **7**, 403–412.
- 36 L. Zhao, T. Bai, H. Wei, J. L. Gardea-Torresdey, A. Keller and J. C. White, Nanobiotechnology-based strategies for enhanced crop stress resilience, *Nature Food*, 2022, **3**, 829–836.
- 37 A. Baxter, R. Mittler and N. Suzuki, ROS as key players in plant stress signalling, *J. Experimental Botany*, 2014, **65**, 1229–1240.
- 38 Y. Yu and M. Flury, Unlocking the Potentials of Biodegradable Plastics with Proper Management and Evaluation at Environmentally Relevant Concentrations, *npj Materials Sustainability*, 2024, **2**, 9, doi:10.1038/s44296-024-00012-0.
- 39 H. A. Leslie, M. J. Van Velzen, S. H. Brandsma, A. D. Vethaak, J. J. Garcia-Vallejo and M. H. Lamoree, Discovery and quantification of plastic particle pollution in human blood, *Environment International*, 2022, **163**, 107199, doi.org/10.1016/j.envint.2022.107199.
- 40 P. Li, Q. Li, Y. Lai, S. Yang, S. Yu, R. Liu, G. Jiang and J. Liu, Direct entry of micro (nano) plastics into human blood circulatory system by intravenous infusion, *Iscience*, 2023, **26**, 108454, doi.org/10.1016/j.isci.2023.108454.
- 41 S. Liu, C. Wang, Y. Yang, Z. Du, L. Li, M. Zhang, S. Ni, Z. Yue, K. Yang, Y. Wang *et al.*, Microplastics in three types of human arteries detected by pyrolysis-gas chromatography/mass spectrometry (Py-GC/MS), *Journal of Hazardous Materials*, 2024, **469**, 133855, doi.org/10.1016/j.jhazmat.2024.133855.
- 42 R. Marfella, F. Prattichizzo, C. Sardu, G. Fulgenzi, L. Graciotti, T. Spadoni, N. D'Onofrio, L. Scisciola, R. La Grotta, C. Frigé *et al.*, Microplastics and nanoplastics in atheromas and cardiovascular events, *New England Journal of Medicine*, 2024, **390**, 900–910.

# Environmental Science Nano

PAPER

Cite this: DOI: 00.0000/xxxxxxxxxx

## Uptake of Polystyrene Nanospheres by Wheat and Arabidopsis Roots in Agar, Hydroponics, and Soil<sup>†</sup>

Kaushik Adhikari<sup>a,b</sup>, Karen A. Sanguinet<sup>b</sup>, Carolyn I. Pearce<sup>c</sup>, Markus Flury<sup>a,b\*</sup>

### Data Availability Statement

All data, including figures and tables, are included in the printed version of the paper.

<sup>a</sup> Department of Crop & Soil Sciences, Puyallup Research & Extension Center, Washington State University, Puyallup, WA 98371, USA.

<sup>b</sup> Department of Crop & Soil Sciences, Washington State University, Pullman, WA 99164, USA.

<sup>c</sup> Pacific Northwest National Laboratory, Richland, WA 99354, USA.

<sup>†</sup> Electronic Supplementary Information (ESI) available: Details on confocal microscopy settings, biomass measurements, statistics, images of polystyrene nanospheres, experimental setups, and confocal z-stack images. See DOI: 00.0000/00000000.